End-to-End Optimal Scheduling for Integrated Energy System with Solid Oxide Fuel Cell

Qiyue Zhu
School of Electrical Engineering
Chongqing University
Chongqing, China
yueqzz314@163.com

Tao Wu
School of Electrical Engineering
Chongqing University
Chongqing, China
taowu.cq@163.com

Kaigui Xie
School of Electrical Engineering
Chongqing University
Chongqing, China
kaiguixie@vip.163.com

Ying Zhang
Department of Electrical and Computer Engineering
Oklahoma State University
Stillwater, U.S.
y.zhang@okstate.edu

Tianqiao Zhao
Department of Electrical Engineering
University of Texas at Arlington
Arlington, U.S
tianqiao.zhao@uta.edu

***Abstract*—Solid oxide fuel cells (SOFCs), known for high efficiency and low emissions, are vital components in integrated energy systems (IESs). However, gas, heat, and electricity dynamics within SOFCs exhibit highly nonlinear relationships, which complicates the scheduling of integrated energy systems. On the other hand, traditional approaches typically separate prediction from decision-making, further compromising the system's operational economy and reliability. To bridge these gaps, this paper proposes an end-to-end optimal scheduling approach for IESs with SOFCs. A linear SOFC model is first developed using two-dimensional piecewise linear approximation techniques. An end-to-end framework integrating load forecasting and system scheduling is then established for IESs with SOFCs. The forecasting module directly targets operational costs minimization by leveraging the cost gradients to update the neural network parameters. Case studies demonstrate that the proposed method achieves up to a 5.65% reduction in average monthly operational costs compared to the traditional methods, while maintaining forecasting accuracy. This result highlights a simultaneous enhancement in both system economics and robustness.**

Keywords*—*integrated energy system, solid oxide fuel cell, end-to-end optimization, load forecasting

I. INTRODUCTION

Integrated energy systems (IESs) represent a pivotal approach to achieving efficient energy utilization and low-carbon development by leveraging multi-energy complementarity. A solid oxide fuel cell (SOFC) is an electrochemical device offering high efficiency, fuel adaptability, and low emissions under medium-to-high temperatures [1]. Furthermore, its capability for cogeneration positions it as a vital distributed power generation technology in IESs, characterized by high energy efficiency and environmental friendliness.

Existing mechanism-level SOFC models [2,3] incorporate multi-physical processes like gas flow, electrochemical reaction, and heat transfer for accurate performance simulation. Ref. [4] constructed an SOFC electrochemical model using the Nernst equation and polarization loss term to reveal the nonlinear current-voltage-energy conversion relationships. Despite their physical depth, the strong non-convex nonlinearity of these models hinders integration into system scheduling. For this reason, some studies simplify the model. Ref. [5] established a linear relationship between hydrogen consumption and power output by setting a fixed conversion ratio. In [6], the nonlinear efficiency relationship between the input hydrogen energy and the output electric and thermal power is described by polynomial fitting. Ref. [7] established an approximate fuel cell model based on the polarization curve, and characterized the output characteristics of the fuel cell stack by the empirical relationship between current, power and hydrogen consumption. However, while linearizing or empirically modeling electrochemical and thermal processes improves computational efficiency, it fails to truly reflect the operational characteristics of SOFC. Therefore, it is urgent to establish an efficient SOFC model that balances modeling accuracy and solution efficiency.

On the other hand, IESs face external uncertainties such as renewable energy and load forecasting errors, which can compromise scheduling economy and safety. To address these challenges, researchers began to explore uncertainty prediction and optimization methods. Regarding prediction, deep learning is widely adopted to improve prediction accuracy. A Copula-DBiLSTM model is constructed in [8] for high-precision multi-load forecasting. Ref. [9] proposed a hybrid neural network with geometric losses within a multi-task framework. Ref. [10] introduced a Bayesian multi-decoder transformer to achieve high-accuracy joint probabilistic forecasting by capturing complex multi-energy coupling relationships. For optimization, existing studies leverage powerful uncertainty methods, such as stochastic programming [11], robust optimization [12], and distributionally robust optimization [13] to hedge against the uncertainties. Based on Latin Hypercube Sampling and K-means clustering, a day-ahead stochastic optimization method for IESs is proposed in [11]. Ref. [12] established a robust optimization model for IESs considering thermal dynamics, utilizing box uncertainty sets to model electrical load and temperature fluctuations. Ref. [13] utilized a two-stage

This work was supported by National Key R&D Program of China (Grant No.2024YFB4007503)

979-8-3315-8138-1

distributionally robust approach with fuzzy sets to enhance system economy. However, as evidenced in [14], enhanced predictive accuracy does not guarantee lower operational costs, and a fundamental distinction exists between the objective of minimizing prediction error and that of optimizing operational cost. In the existing research, load forecasting and scheduling optimization are handled separately based on "forecasting-then-optimization (FTO)". This framework fails to coordinate forecasting and decision-making under the guidance of operating cost. Consequently, such forecasting results cannot be fully leveraged to enhance the system operation economy.

In view of the above research deficiencies, this paper proposes an end-to-end optimal scheduling approach for IESs with SOFCs. The main contributions are as follows:

1) A linear SOFC model is developed. The nonlinear non-convex output power surface of the SOFC is approximated using two-dimensional piecewise linear fitting, enabling its efficient integration into system dispatch.

2) An end-to-end optimization framework integrating load forecasting and system scheduling is established. Through the back-propagation of cost gradients, the prediction model updates parameters with the goal of minimizing operating costs, which significantly improves the system economy.

II. IES Structure and Refined Modeling of SOFC

A. IES Framework

The IES established in this paper is based on the energy hub model, as shown in Fig. 1. Electric load sources include the upstream power grid, wind power and photovoltaics, combined heat and power (CHP), SOFC, and electrical storage (ES). Thermal load sources comprise gas boilers (GB), CHP, SOFC, and thermal storage (HS).

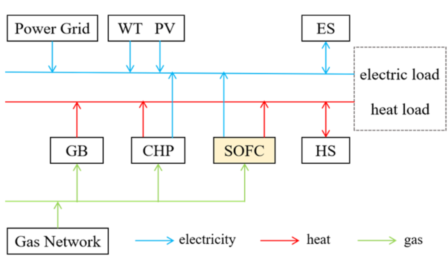

Fig. 1. Structure of integrated energy system based on energy hub model.

B. SOFC Gas-Heat-Electricity Coupling Model

The current represents the rate of charge transfer, and the magnitude of current flowing through the SOFC I_{cell} is proportional to the molar flow rate w. The output voltage of a single SOFC cell V_{cell} is determined by summing all voltage contributions, comprising four components: the Nernst voltage E_{nernst}, ohmic loss voltage V_{ohm}, activation loss voltage V_{act}, and concentration difference loss voltage V_{con}. The specific mathematical model is as follows:

$$I_{cell} = 2F \cdot w \tag{1}$$

$$V_{cell} = E_{nernst} - V_{ohm} - V_{act} - V_{con} \tag{2}$$

$$E_{nernst} = E^0 - k_E (T - T_0) - \frac{RT}{2F} \ln \frac{p_{H_2O}}{p_{H_2} p_{O_2}^{0.5}} \tag{3}$$

$$V_{ohm} = \left[(\rho_{an} \cdot \tau_{an} + \rho_{el} \cdot \tau_{el} + \rho_{ca} \cdot \tau_{ca}) / S \right] \cdot I_{cell} \tag{4}$$

$$\rho_{el} = \frac{1}{33.4 \times 10^3 \exp(\frac{-10.3 \times 10^3}{T})} \tag{5}$$

$$V_{act} = \frac{RT}{F} \sin^{-1}(\frac{i}{2i_{0,an}}) + \frac{RT}{F} \sin^{-1}(\frac{i}{2i_{0,ca}}) \tag{6}$$

$$V_{con} = \frac{RT}{2F} \ln \frac{i_L}{i_L - i} \tag{7}$$

where E^0 denotes the reversible voltage of the fuel cell under standard conditions, k_E is a constant, T is the cell temperature, and $p_{H_2}, p_{O_2}, p_{H_2O}$ denote the dimensionless partial pressures of hydrogen, oxygen, and water vapor, respectively; $\rho_{an}, \rho_{ca}, \rho_{el}$ and $\tau_{an}, \tau_{ca}, \tau_{el}$ denote the resistivity and thickness of the anode, cathode, and electrolyte, respectively; i, $i_{0,an}/i_{0,ca}$, i_L represent the current density, exchange current density, and limiting current density, respectively.

The power output of a fuel cell stack is the product of the number of individual cells, the output voltage per cell, and the stack current. During SOFC operation, a significant portion of the energy is released as heat due to voltage losses. Its electrical power and thermal power can be calculated as:

$$P = N \cdot V_{cell} \cdot I_{cell} \tag{8}$$

$$Q = N \cdot (E_{nernst} - V_{cell}) \cdot I_{cell} \tag{9}$$

C. Linearization of the SOFC Model

The gas molar flow rate, temperature, and power output of SOFC power generation units exhibit a nonlinear relationship. Their refined model mathematically represents a non-convex nonlinear model with high computational complexity, making it difficult to solve efficiently during scheduling.

This paper employs a two-dimensional piecewise linear approximation technique. First, the two-dimensional operating domain $(t, w)$of the SOFC is divided into $N_t \times N_w$ rectangular blocks. For the block k, its boundaries are $[t_k^{min}, t_k^{max}]$and $[w_k^{min}, w_k^{max}]$. By performing dense sampling within each block, the actual power output is obtained. Subsequently, using the least squares method, optimal linear approximation planes for both P_e and Q_h are fitted for each block k.

$$\begin{cases} P_{e,k}(t,w) \approx a_p^k \cdot t + b_p^k \cdot w + c_p^k \\ Q_{h,k}(t,w) \approx a_q^k \cdot t + b_q^k \cdot w + c_q^k \end{cases} \tag{10}$$

During the optimization phase, the precomputed K linear blocks are embedded into the MILP model. The core approach involves introducing a set of binary variables $z_{i,t,k}$ $(k = 1,2,\dots,K)$ for each SOFC at time t, using the constraint $\sum_{k=1}^{K} z_{i,t,k} \leq 1$ to ensure that at most one SOFC operates within a given operating region at time t. Simultaneously, interval constraints enforce that the operating point (t, w) of the SOFC must lie within the valid boundary of its assigned block. Subsequently, the linear equation $P_e = a_p^k \cdot t + b_p^k \cdot w + c_p^k$ fitted to this block is used to calculate its electrical power (thermal power follows similarly).

979-8-3315-8138-1

Through this transformation, the nonlinear, non-convex model of the SOFC is successfully and accurately converted into a set of MILP constraints, enabling it to be processed by a linear optimization solver.

III. END-TO-END OPTIMIZATION

A. Load Forecasting Module

LSTM is employed as a load forecasting model, which is a recurrent neural network that captures long-term and temporal dependencies through specialized gating units. Its prediction process primarily relies on three distinct gates: the forget gate F, the input gate I, and the output gate O. The forget gate determines which information should be discarded from the previous memory cell $c(t-1)$. The input gate determines how much of the information from the input at time t should be stored in the current memory cell $c(t)$. The output gate controls how much information is deemed valuable to be considered as the model's output.

The input features received by this model include historical load data, calendar features, and weather features, ultimately outputting load forecast values for 24 time points on the following day .

B. System Scheduling Module

The dispatch module establishes the IES Low-Carbon Economy Dispatch Model, with an objective function to minimize total operating costs encompassing energy procurement costs, tiered carbon trading costs, operation and maintenance costs, and penalties for curtailed wind and solar power. Details are as follows:

$$\min C_{total} = C_{buy} + C_{co_2} + C_{O\&M} + C_{curt} \tag{11}$$

$$C_{buy} = \sum_{t=1}^{T} \left(c_{e,t}^{buy} P_{e,t}^{buy} + c_{g}^{buy} P_{g,t}^{buy} + C_{H_2,t}^{prod} \right) \tag{12}$$

$$C_{CO_2} = \begin{cases} c \cdot E_{gap} & E_{gap} \le l \\ lc + c(1+k)(E_{gap} - l) & l \le E_{gap} \le 2l \\ (2+k)lc + c(1+2k)(E_{gap} - 2l) & 2l \le E_{gap} \le 3l \\ (3+3k)lc + c(1+3k)(E_{gap} - 3l) & 3l \le E_{gap} \le 4l \\ (4+6k)lc + c(1+4k)(E_{gap} - 4l) & E_{gap} \ge 4l \end{cases} \tag{13}$$

$$C_{O\&M} = \sum_{t=1}^{T} \sum_{k \in \Omega} c_{om,k} P_{k,t} \tag{14}$$

$$C_{curt} = \sum_{t=1}^{T} c_{curt} \left(P_{WPV,t}^{\max} - P_{WPV,t} \right) \tag{15}$$

In order to ensure the safe and reliable operation of the system, the above low-carbon economic dispatch model considers equipment climbing, wind and solar output, energy storage operation constraints, energy balance constraints, and SOFC linearization constraints mentioned in the previous section. Some of the important constraints are:

$$\begin{cases} 0 \le P_{ES}^{cha/dis}(t) \le \xi_{ES}^{cha/dis}(t) P_{ES}^{\max} \\ S_{ES}(t) = S_{ES}(t-1) + P_{ES}^{cha}(t)\eta_{ES}^{cha} - P_{ES}^{dis}(t) / \eta_{ES}^{dis} \\ S_{ES}(T) = S_{ES}(1),\ S_{ES}^{\min} \le S_{ES}(t) \le S_{ES}^{\max} \\ \xi_{ES}^{cha}(t) + \xi_{ES}^{dis}(t) = 1 \end{cases} \tag{16}$$

$$P_{e,buy}(t) + P_{WPV}(t) + P_{CHP,e}(t) + P_{SOFC,e} = P_{e,load}(t) + P_{ES}(t) \tag{17}$$

$$P_{CHP,h}(t) + P_{GB,h}(t) + P_{SOFC,h} = P_{h,load}(t) + P_{HS}(t) \tag{18}$$

$$P_{g,buy}(t) = P_{g,GT}(t) + P_{g,GB}(T) + P_{g,SOFC} \tag{19}$$

C. End-to-End Modeling

The end-to-end model training framework is illustrated in Fig.2. The load forecasting module is deeply coupled with the economic dispatch module to achieve joint optimization targeting the minimization of total system operating costs. This process comprises two core stages: forward propagation for solution and backward propagation for updates.

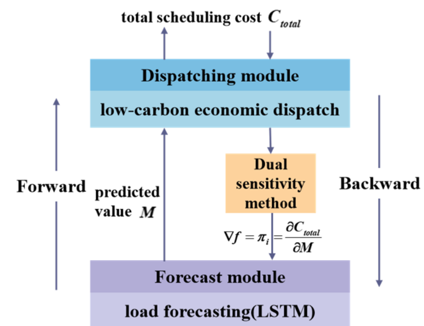

Fig. 2. End-to-End framework for integrated forecasting and scheduling.

The objective of the forward propagation phase is to solve the complete economic dispatch problem based on the current forecast from the prediction module, thereby obtaining daily operating costs and optimal integer decisions. The objective of the backward propagation phase is to compute the gradient of total cost C_{total} with respect to the forecast value M, and propagate this gradient backward to update the parameters ω of the prediction model.

The system scheduling model introduces block-linearized decision variables to approximate the nonlinear relationships of SOFCs, along with mutually exclusive binary variables in the energy storage charging/discharging constraints. Due to the integer variables in the MILP problem causing the objective function to be discontinuous and non-differentiable with respect to predicted values, the scheduling problem cannot be simply differentiated. Therefore, we employ a two-stage solution. We use the integer solution obtained in the forward phase to fix all integer variables in the original MILP problem. This operation reduces the complex MILP problem to a pure, differentiable linear programming (LP) subproblem. After that, the dual sensitivity method is used to calculate the gradient. Based on the dual theory of linear programming, the sensitivity (i.e., gradient) of the optimal target value of the LP problem to the right side of its constraint (i.e., the load forecast value in our model) is exactly equal to the optimal dual variable of the constraint. We solve the LP subproblem and extract the corresponding dual variables. Therefore, the cost gradient we need is:

$$\nabla f = \frac{\partial C_{total}}{\partial M} = \pi_i \tag{20}$$

Although fixing integer variables during backpropagation neglects discrete differentiation, this approximation is theoretically grounded and has been applied in recent studies [15]. Mathematically, this method essentially treats gradient calculation as a sensitivity analysis of the optimal linear sub-problem at the optimal solution. According to differentiable optimization theory [16], once the optimal discrete mode is determined by the forward pass, the local sensitivity of the objective function with respect to the forecasts is primarily dominated by the continuous variables. From the perspective of convergence, given that the loss landscape of MILP problems is inherently discontinuous and non-differentiable, fixing integer variables effectively constructs a piecewise smooth surrogate surface. This avoids gradient oscillations caused by discrete jumps and ensures a stable gradient descent direction.

By iteratively executing these two stages on the training data set, the prediction model is gradually fine-tuned, so that its parameters are no longer optimized only to minimize the prediction error, but directly to minimize the operating cost of the downstream economic dispatch module.

IV. Case Study

To verify the effectiveness and superiority of the proposed end-to-end optimization method, the IES shown in Fig. 1 is used for example testing. The data of electricity, heat load and meteorological characteristics are from the data set of Arizona State University, of which 2022 is the training set and 2023 is the test set. The scheduling module takes 24 h as a cycle and the time step is 1 h. The experiments in this work were conducted in the virtual environment of Python 3.9.19 and Pytorch 2.0.1.

A. End-to-End Optimization Results

As shown in Table I, the end-to-end optimization method demonstrates consistent cost improvement across all months of the year. Compared to the traditional FTO approach, the system achieves monthly average operational cost reductions ranging from 4.25% to 5.65% under end-to-end training. This indicates that end-to-end optimization effectively reduces system operating costs across different seasons and load levels, ensuring consistent and sustainable economic gains throughout the year.

Fig. 3 further illustrates the distribution of daily operating costs throughout the year. It is evident that the cost distribution under the end-to-end approach is generally lower than that of the traditional FTO method, with a significantly reduced median, narrower interquartile range, and fewer high-cost outliers. This indicates that end-to-end optimization effectively reduces mean costs while mitigating extreme high-cost scenarios, leading to smoother and more reliable operation. In short, the collaborative training of forecasting and scheduling significantly enhances both the economic efficiency and stability of IESs.

TABLE I. Comparison of Average Daily Operating Costs by Month

Month	FTO (CNY)	End-to-End (CNY)	Improvement
Jan.	62136.08	59497.15	4.25%
Feb.	58689.25	55875.20	4.79%
Mar.	48310.25	45812.14	5.17%
Apr.	47418.88	44953.60	5.20%
May	78351.82	74032.04	5.51%
Jun.	83344.20	78973.03	5.24%
Jul.	122802.28	116799.26	4.89%
Aug.	120987.89	115069.09	4.89%
Sep.	107594.96	102227.56	4.99%
Oct.	80225.92	75690.74	5.65%
Nov.	66345.10	62811.14	5.33%
Dec.	49226.51	46483.00	5.57%

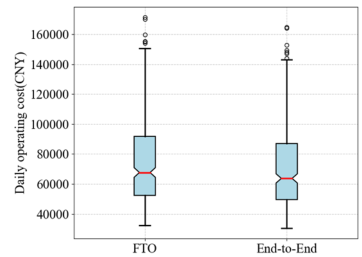

Fig. 3. Comparison of annual daily operating cost distributions.

As shown in Table II, the changes in load prediction accuracy before and after end-to-end training are minimal, with overall performance remaining stable. The mean absolute error (MAE) and mean absolute percentage error (MAPE) for electrical load predictions show slight improvements, while thermal load prediction accuracy has decreased marginally but still maintains a low error rate. This indicates that the end-to-end optimization framework achieves a significant reduction in system operating costs without compromising prediction performance.

TABLE II. Comparison of Load Forecasting Accuracy

	Model	MAE	MAPE
Electric load	Basic	622.105	8.43%
	End-to-End	619.80	8.19%
	Accuracy variation	0.37%	2.85%
Heat load	Basic	109.42	6.01%
	End-to-End	115.38	6.26%
	Accuracy variation	-5.44%	-4.16%

The generalizability of the proposed end-to-end method is validated by adjusting the peak-to-valley price spread scaling factor K_{PRICE} and the renewable energy penetration scaling factor K_{WPV}. Across all test scenarios, the operating costs of the end-to-end method are consistently lower than those of the traditional FTO approach, with its advantages becoming more pronounced under volatile price fluctuations or high-proportion renewable energy integration. These results demonstrate that the end-to-end framework effectively synchronizes forecasting and decision-making, offering greater economic robustness and adaptability than FTO in volatile environments.

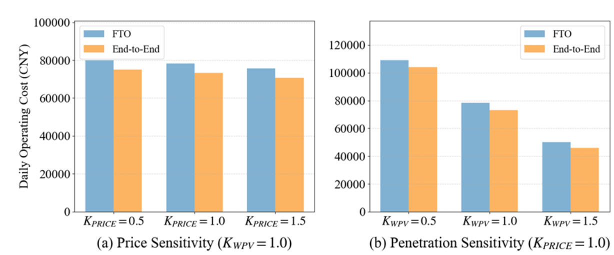

Fig. 4. Sensitivity analysis of daily operating costs under different scenarios.

B. Analysis of the End-to-End Training Process

Fig. 5 illustrates the evolution of operating costs and load forecasting normalized mean square error (MSE) over training iterations. The steady decline in costs for both training and test sets confirms the model's effectiveness. The MSE reaches a minimum plateau between Epochs 4 and 6 before rebounding

979-8-3315-8138-1

sharply, signaling a significant loss in prediction accuracy. Consequently, selecting the model at the Epoch 6 elbow point achieves a Pareto optimal balance between forecasting fidelity and systemic economy.

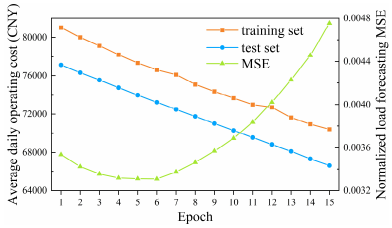

Fig. 5. Evolution of operating cost and normalized forecasting MSE over training epochs.

The electric and thermal load balance analysis in Fig. 6 shows that the end-to-end model effectively reduces purchased electricity and equipment ramping pressure through SOFC peak-shaving and energy storage "low-charge, high-discharge" operations. This proves that the end-to-end framework leverages "strategic" forecasting to guide the optimizer, enhancing SOFC/CHP efficiency while significantly lowering operational costs through efficient peak-shaving and valley-filling.

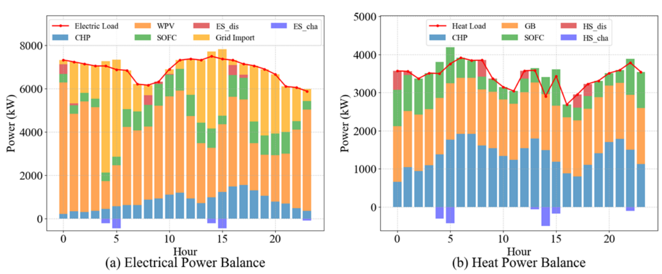

Fig. 6. Optimal electric and heat dispatch on typical spring day.

Table III compares the computational efficiency of the traditional FTO and the proposed end-to-end methods. During offline training, the end-to-end approach incurs a significantly higher per-epoch execution time than FTO, as it invokes a MILP solver during the forward pass of each iteration to integrate downstream scheduling costs into the network weights. Although integer variables increase the complexity of forward scheduling, the dual-theory-based analytical gradient method transforms backpropagation into a linear programming problem, preventing exponential growth in computational burden. Once trained, the model's online execution time remains on the same order of magnitude as FTO, fully meeting the real-time requirements of IES scheduling.

TABLE III. COMPARISON OF COMPUTATIONAL EFFICIENCY

Method	Offline training time (s/epoch)	Online execution time (s/day)
FTO	39.29	7.21
End-to-End	588.95	14.17

V. CONCLUSION

This paper proposes an end-to-end optimization scheduling method for IESs with SOFCs. A two-dimensional piecewise linear approximation approach is first employed to convert the complex nonlinear SOFC model into efficient mixed-integer linear constraints. Second, an integrated forecasting-scheduling architecture is constructed. Dual sensitivity analysis feeds back cost gradients to drive the forecasting model toward minimizing operational costs, achieving synergy between prediction and decision-making. Case studies show that the proposed approach achieves an average cost reduction of approximately 5.12% compared to FTO, while maintaining forecasting accuracy. The more concentrated cost distribution and fewer high-cost extremes also indicate enhanced operational robustness.

REFERENCES

[1] J. Peng, J. Huang, X. Wu *et al*.,"Solid oxide fuel cell (SOFC) performance evaluation, fault diagnosis and health control: A review," Journal of Power Sources, vol. 505, pp. 230058, 2021.

[2] J. Zhang, P. Cui, S. Yang *et al*., C. Deng, and S. Wang, "Thermodynamic analysis of SOFC–CCHP system based on municipal sludge plasma gasification with carbon capture," Applied Energy, vol. 336, pp. 120822, 2023.

[3] Z. Shao, X. Cao, Q. Zhai, and X. Guan, "Risk-constrained planning of rural-area hydrogen-based microgrid considering multiscale and multi-energy storage systems," Applied Energy, vol. 334, pp. 120682, 2023.

[4] C. Shen, W. Gu, and X. Shen, "Grid-forming control for solid oxide fuel cells in an islanded microgrid using maximum power point estimation method," IEEE Transactions on Sustainable Energy, vol. 15, no. 3, pp. 1703–1714, July 2024.

[5] X. Fang, W. Dong, Y. Wang, and Q. Yang, "Multiple time-scale energy management strategy for a hydrogen-based multi-energy microgrid," Applied Energy, vol. 328, pp. 120195, 2022.

[6] J. Zhang and Z. Liu, "Low carbon economic scheduling model for a park integrated energy system considering integrated demand response, ladder-type carbon trading and fine utilization of hydrogen," Energy, vol. 290, pp. 130311, 2024.

[7] T. Li, H. Liu, H. Wang, and Y. Yao, "Hierarchical predictive control-based economic energy management for fuel cell hybrid construction vehicles," Energy, vol. 198, pp. 117327, 2020.

[8] J. Zheng, L. Zhang, J. Chen *et al.*, "Multiple-load forecasting for integrated energy system based on Copula-DBiLSTM," Energies, vol. 14, no. 8, pp. 2188, 2021.

[9] P. Zhao, D. Cao, W. Hu *et al.*, "Geometric loss-enabled complex neural network for multi-energy load forecasting in integrated energy systems," IEEE Transactions on Power Systems, vol. 39, no. 4, pp. 5659–5671, 2024.

[10] C. Wang, Y. Wang, Z. Ding, and K. Zhang, "Probabilistic multi-energy load forecasting for integrated energy system based on Bayesian transformer network," IEEE Transactions on Smart Grid, vol. 15, no. 2, pp. 1495–1507, 2024.

[11] F. Mei, J. Zhang, J. Lu, Y. Jiang, J. Gu, K. Yu, and L. Gan, "Stochastic optimal operation model for a distributed integrated energy system based on multiple-scenario simulations," Energy, vol. 219, pp. 119629, 2021.

[12] S. Lu, W. Gu, S. Zhou, S. Yao, and G. Pan, "Adaptive robust dispatch of integrated energy system considering uncertainties of electricity and outdoor temperature," IEEE Transactions on Industrial Informatics, vol. 16, no. 7, pp. 4691–4702, 2020.

[13] Y. Qiu, Q. Li, Y. Ai *et al.*, "Two-stage distributionally robust optimization-based coordinated scheduling of integrated energy system with electricity–hydrogen hybrid energy storage," Protection and Control of Modern Power Systems, vol. 8, p. 33, 2023.

[14] J. Zhang, Y. Wang, and G. Hug, "Cost-oriented load forecasting," Electric Power Systems Research, vol. 205, pp. 107723, 2022.

[15] Y. Zhou, Q. Wen, J. Song *et al*, "Load Data Valuation in Multi-Energy Systems: An End-to-End Approach," IEEE Transactions on Smart Grid, vol. 15, no. 5, pp. 4564–4575, 2024.

[16] B. Amos and J. Z. Kolter, "OptNet: Differentiable optimization as a layer in neural networks," Proceedings of the 34th International Conference on Machine Learning, vol. 70, pp. 136–145, 2017.